IDENTIFICATION OF BEARING HOUSING VIBRATIONS OF A LARGE BARREL TYPE INJECTION PUMP AND THEIR ANALYSIS BY MEANS OF THE FINITE ELEMENT METHOD

by

Wolfram Lienau

Manager Analysis and Mechanics

Sulzer Pumps Ltd.

Winterthur, Switzerland

Peter Sandford

Technical Services Manager

Sulzer Pumps (UK) Ltd.

GB-Leeds, United Kingdom

and

Yasar Deger

Senior Engineer/Expert in Structural Mechanics

Sulzer Innotec

Winterthur, Switzerland

Wolfram Lienau is Manager of the Analysis and Mechanics group of Sulzer Pumps Ltd., in Winterthur, Switzerland. After three years working as a teaching assistant at the technical university in Darmstadt, Germany, he joined the R&D division of Eastman Christensen, a drilling tool manufacturer. Mr. Lienau's activities included the strength calculation of drilling tools, components of them, and the mechanical behavior of drill pipes, mainly by means of finite element analyses. In 1990, he moved to Sulzer Innotec as the head of the Structural Mechanics group. In 2000, Mr. Lienau joined Sulzer Pumps. Mr. Lienau is also engaged as lecturer at the Mechanical Engineering Department of ZHW, University of Applied Sciences, Winterthur, Switzerland, where he teaches strength of materials.

Mr. Lienau studied at the technical university in Braunschweig, Germany, where he received his Master diploma in Mechanical Engineering.

Peter Sandford is Technical Services Manager at Sulzer Pumps (UK) Ltd., providing support on noise, vibration, and related matters to the Sales, Projects, and Service Departments. After five years at the R&D Department of David Brown Gears, working in the field of noise and vibration, Mr. Sandford transferred to the Bingham Pump division in 1978 to pursue similar activities. His work at DB-Bingham at this time included investigations into the phenomenon of acoustic resonance in centrifugal pumps. He took the position of R&D Engineer at a generating set manufacturer in 1989, rejoining DB-Pumps in 1991 to resume responsibility for rotordynamics, instrumentation, noise, and vibration. This work also concerned support for service/commissioning onsite, the development of machinery vibration standards, and participation in an international R&D project to develop a machinery condition monitoring system. He joined Sulzer Pumps in 2002.

Mr. Sandford graduated with a B.Eng. degree from Liverpool University (1972).

Yasar Deger is Senior Engineer/Expert in Structural Mechanics at Sulzer Innotec, the R&D facility of Sulzer Corporation, which he joined in 1998. His activities cover thermal, static, and dynamic finite element (FE) analyses for a wide range of industrial applications, with a special interest in structural dynamics and on updating of FE models based on results of experimental modal analysis. Dr. Deger is also engaged as lecturer at the Mechanical Engineering Department of HSR, University of Applied Sciences, Rapperswil, Switzerland, where he has taught Engineering Mechanics and Finite Element Method since 1979.

Dr. Deger received his Ph.D. in 1981 at the ETH, Swiss Federal Institute of Technology, in Zurich. Before his affiliation with Sulzer Innotec, he collected professional experiences at several institutions, e.g., Swiss Association of Technical Inspections/Nuclear Division, former Sulzer Division of Thermal Energy Systems, Swiss Federal Laboratories of Materials Testing and Research.

ABSTRACT

It should be an objective to predict bearing housing vibrations by means of finite element methods and avoid them in the design phase rather than to go in for corrective actions on the test bed or in the field. Bearing housing vibrations due to an excitation by the impeller vanes occur, if there is a natural frequency of the pump. The finite element method is a useful tool to determine natural frequencies, but it is still necessary to compare them with real tested structures. Especially the connecting stiffness between different parts in a structure and the boundary conditions has often to be estimated. Within this paper the determination of bearing housing frequencies has been undertaken systematically from a simple test device to a complete barrel pump.

With the test device several influences onto the natural frequencies were studied, such as internal pressure, bolting, seals, and foundation stiffness. It is demonstrated that with appropriate

modeling and assumptions the measured frequencies can be accurately met by means of finite elements. The rules observed were applied to a full 3-D model of a barrel pump. The natural frequencies were determined by means of this finite element model. An experimental modal analysis was carried out on the real structure of this pump assembly. At several locations of the surface transducers were placed and the response due to the hammer test was identified in terms of frequencies and modal shapes. This result was correlated with the finite element results to update the finite element model and obtain better congruence between experiment and analysis. The results were promising, especially for the most important bearing housing natural frequency, where the differences between analysis and test were very low. This gives confidence to future analyses of bearing housing vibrations.

INTRODUCTION

Bearing housing vibrations of pumps are difficult to predict, if the excitation is due to vane passing frequency. On the other hand pump manufacturers have to guarantee certain vibration limits of their pumps, measured at these bearing housings. These limits are given in different standards, e.g., API 610, Ninth Edition (2003), requires a maximum vibration limit of 3 mm/s root-mean-square (rms) for a newly commissioned pump. The excitation frequencies of interest depend on speed and the number of impeller vanes and are in general between 250 Hz at 3000 rpm and five vanes, and 700 Hz at 6000 rpm and seven vanes. They are calculated by dividing the rpm-speed by 60 and multiplying it by the number of impeller vanes. In this frequency range the pump assemblies might show natural frequencies at the bearing housings. If the excitation frequency equals the natural frequency a resonance situation with high vibration amplitudes occurs, which is above the limits. In this case expensive measures have to be carried out to reduce the vibrations, either by reducing the excitation amplitude or by shifting the natural frequency by design measures. Due to this reason advance knowledge of the bearing housing natural frequencies is of importance during the design phase.

The finite element method can be a useful tool in predicting these bearing housing vibrations. The difficulties in using this tool are the definition of precise boundary conditions and the modeling of the different assembly parts with their interfaces affected by the vibration. Parts may be clamped together by bolts, there may be a seal in between, or they are fitted together by a loose fit or an interference fit. The fluid, seals and gaskets, and others provide damping of unknown quantity. With the investigated barrel pump design the drive-end at the suction side is more complex than the nondrive-end. Another difficulty is to distinguish between standstill and operating conditions, where the internal pressure changes the contact stiffness between the different parts.

The influence of all these mostly unknown parameters was experimentally determined with a simplified test device modeled after the drive-end of a pump. The test device was tapped with an instrumented hammer to measure its natural frequencies. The natural frequencies and mode shapes were then modeled with a finite element model and compared.

With the knowledge of the results obtained a refined finite element model of a complete injection barrel pump was created and its natural frequencies determined by means of finite elements. The bearing housing vibrations occur simultaneously at the drive-end and nondrive-end in-phase and with higher frequency out-of-phase in the horizontal and vertical direction. The foundation stiffness at the pump feet has an important influence on the bearing housing frequencies and amplitudes. At this manufactured pump (Figure 1) hammer tests were again performed at the pump mounted in the test bed and the eigenvalues were determined experimentally. The measurement points were placed according to the results of the finite element analysis. The experimental results were then correlated with the analysis results by means of specialized software. The whole procedure as it should be is shown in

Figure 2 (Dascotte, 2004). The correlation was fairly good and could be improved by modifying parameters of the finite element model.
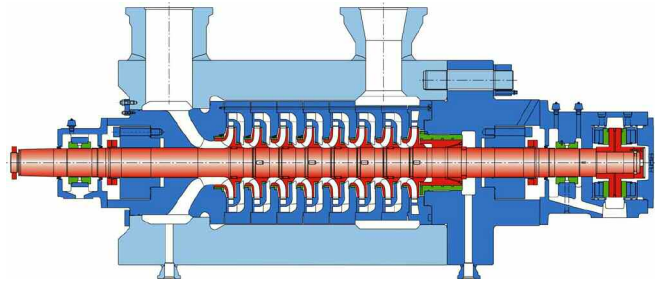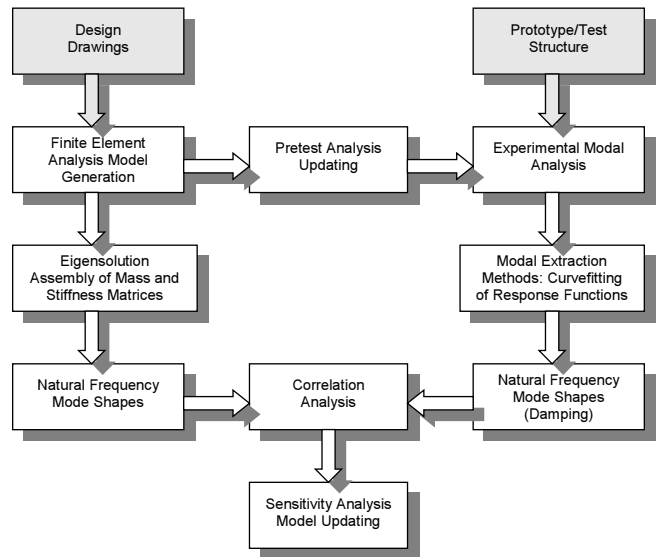

Figure 1. Injection Pump.

Figure 2. Procedure for Linking Test and Analysis in Modal Analysis.

The detailed analysis of the bearing housing vibrations showed that their vibration is not a problem of the bearing housing structure alone. Depending on the mode shapes the structure of the whole pump is involved in the vibration. The bearing housing vibration can react with each other, this means that, i.e., a vertical drive-end (DE) vibration is in-phase with a nondrive-end (NDE) vibration or might have a phase of 180 degrees. To predict these phenomena, a minimum of modeling of the pump is necessary. This depends on the pump design and the bearing housing considered—DE or NDE. For future applications the prediction is much easier with the knowledge of this analysis and corrective measures can be made in advance.

TEST DEVICE

Tests

In a first step a test device was designed and manufactured (Figures 3 and 4). The test device geometry is similar to the drive-end of a barrel pump. Onto a baseplate, 013, the outer barrel, 002, is bolted and the suction casing, 001, is welded onto this plate. A clamping ring, 003, connects both. Either an O-ring seal, 012, or a graphite seal, 010, can be inserted in between. A kind of bearing housing, 004, with a cap, 005, is flanged to the suction casing. The test device was designed in a way that its natural frequencies are about 500 Hz when clamped to a rigid foundation. For the purpose of design, finite element models were created and varied in their geometry, until this goal was reached. The test device allows a lot

IDENTIFICATION OF BEARING HOUSING VIBRATIONS OF A LARGE BARREL TYPE
INJECTION PUMP AND THEIR ANALYSIS BY MEANS OF THE FINITE ELEMENT METHOD

3

of modifications: the seal could be either an O-ring or a graphite profile seal or no seal could be inserted. The number of bolts 007, 008, and 009 could easily be modified at each flange. It could be internally pressurized by water. The flange toward the end could be either smooth or milled between the boltholes. Accelerometers are attached at the different positions in the two lateral directions as well as the vertical direction of the test device to obtain the mode shapes of it.
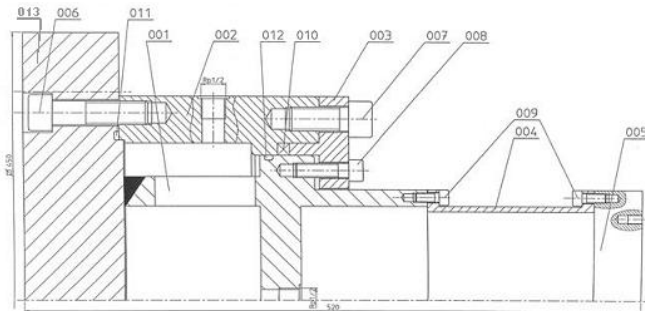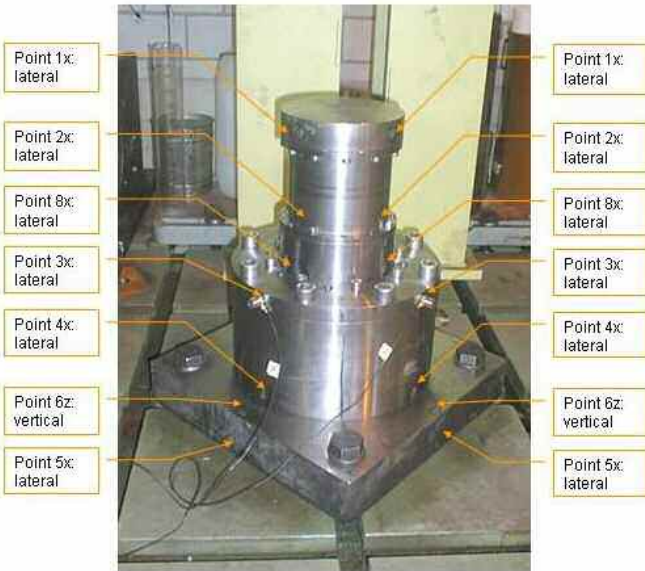

Figure 3. Test Device Schematic.

Figure 4. Test Device Photo.

For the experimental modal analysis, the response characteristic between an exciting force and the resulting accelerations in different points of the structure is determined. The global parameters natural frequency and modal damping as well as the local components of the mode shapes, the eigenvectors, can be derived from the response characteristics. In this case the "single input, multiple output method" with locally fixed excitation has been used. An impact hammer with an integrated force transducer has excited the test device. The driving point has been chosen on the cap, 005, the area of the highest bending amplitudes. The hammer impact direction was chosen perpendicular to the rotational symmetry axis. The structural model for the experimental modal analysis was composed of straight beams (wire frame model) tracking bending eigenvalue shapes (lateral movements) and the baseplate movement in the symmetry axis direction (Figure 5). The extraction of natural frequencies has been focused on the proper determination of the first bending modes, the deepest natural oscillations occurring at approximately 500 Hz.

A test program with 34 combinations of these features was performed. Table 1 shows the test parameters selected. Not all combinations are possible.
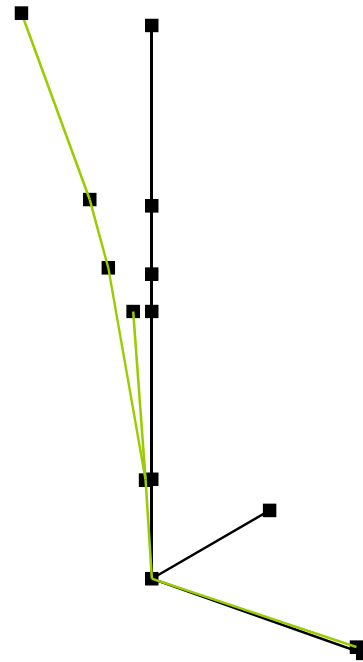

Figure 5. Experimental Modal Analysis.

Table 1. Test Parameters.

Flange 004	Sealing	Medium / Pressure	# of bolts 009	# of bolts 008
Smooth	none	none	12	16
milled	O-Ring	Water 20 bar	6	12
	Graphite profile seal		4	8
				4
				0

Evaluations were made according to the combined features; the Figures 6, 7, and 8 show selected results. Variations in the results of 1 percent or approximately 5 Hz are within measurement accuracy. Parameters with such variations can be neglected. Figure 6 shows that the O-ring sealing only has a negligible influence on the natural frequencies. It shows as well that the influence of the annulus fluid film under internal pressure is negligible as well. The milling of the flange also has no significant effect. The reason is the geometry of this flange, which allows—as if the flange would be not milled—only local contact in the bolt region. Everywhere else a contact opening occurs similar to the milled flange. The damping values for the first bending mode are all very small (mean value 1.68 percent); in general the damping values are below 2 percent: only very few test configurations produced a higher damping value. The damping influence on the natural frequencies can be neglected as well.
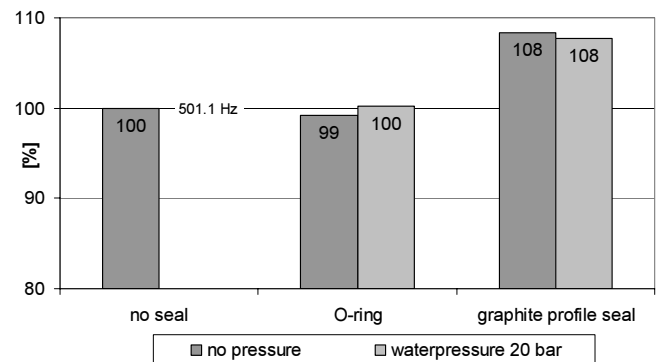

Figure 6. Influence of Seal Type and Internal Pressure onto the Natural Frequencies.
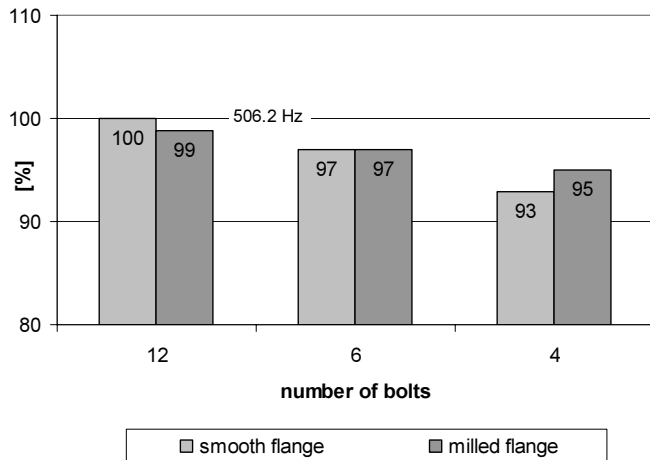
Figure 7. *Influence of Flange Type and Number of Flange Bolts onto the Natural Frequencies.*
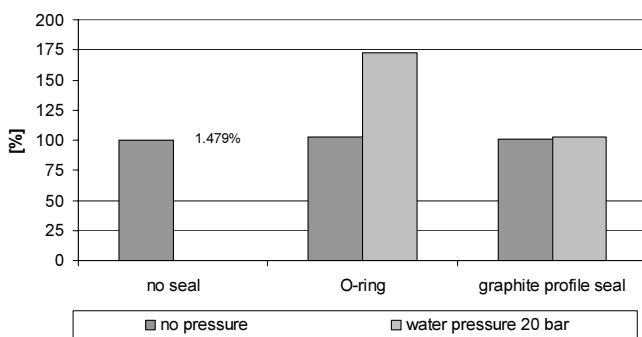

Figure 8. *Influence of Seal Type and Internal Pressure onto the Damping.*

Other parameters have a significant influence. These are first the numbers of bolts, especially at the flange simulating the bearing housing connection 009. The graphite profile sealing increases the natural frequencies significantly and has an influence as well. Last but not least the way the test device is mounted onto the bed with its baseplate was a very important factor. Especially this last point showed that a modeling of the bearing housing vibration by finite elements could not stop at the suction casing; the barrel has to be taken into account as well.

Simulation

The test device was simulated by means of the finite element method (Figure 9). Linear brick elements plus some wedge elements were used; this simple geometry allows this kind of modeling and the model contains about 55,000 elements with 65,000 nodes. Normal structural steel material data for the Young's modulus, the Poisson ratio, and the density were applied. The boundary conditions are fixations at the locations of the four bore holes of the baseplate, or at the beam elements applied at these bores to simulate the fixation bolts.

As the bolted connections were important in the test device, the way of modeling these bolts was an essential issue. Two different types of bolts are included in the test device: with and without a free clamping length. At the clamping ring the bolts toward the suction casing have a free length and, as there is no contact between clamping ring and suction casing, the bolt can be modeled by beam elements with the associated bolt diameter. At all other bolted connections there is contact between the parts. The VDI Standard 2230 (2003) defines an equivalent diameter according to the compressed area (Figure 10) to define the flange stiffness. An area of this diameter is used to merge the parts together in the analysis. Due to the brick elements a square area of the elements around the bolting location approaches this.
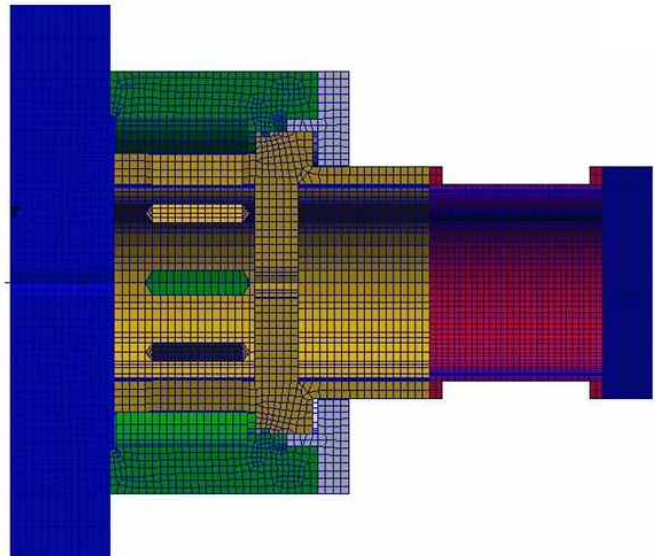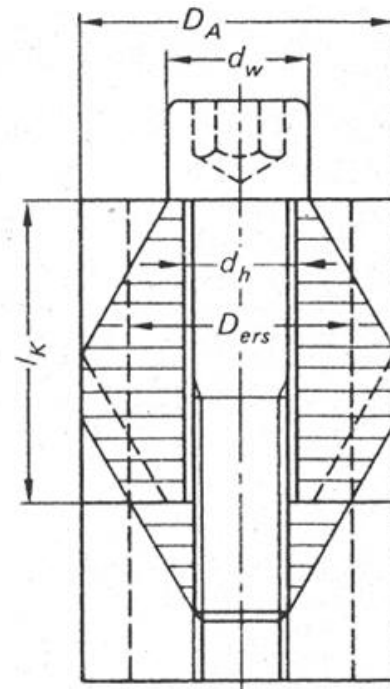

Figure 9. *Finite Element Model Test Device.*

Figure 10. *Equivalent Flange Diameter D_{ers}.*

Another task was the modeling of the graphite profile seal. It was simulated by elements with a linear material behavior. The modulus of elasticity and Poisson ratio had to be adapted to the compressed state of the seal. Material data from the seal manufacturer had been used to evaluate this property.

For the analysis damping is neglected. This means that the finite element program computes only real eigenvalues. Table 2 shows a comparison between the tests and the simulations of the first and most interesting eigenvalue. The baseplate bolts were calibrated by their stiffness to the test with no seal; no pressure and no clamping ring bolts (test #5). Their stiffness was found to be the quadruple of the single bolt tensile stiffness. This is in accordance with Dascotte (2004). There is a good agreement between the measured frequencies and the calculated. With the applied modeling techniques, analysis and test differed only a little bit. This shows that modeling in the way described above leads to the correct results.

IDENTIFICATION OF BEARING HOUSING VIBRATIONS OF A LARGE BARREL TYPE
INJECTION PUMP AND THEIR ANALYSIS BY MEANS OF THE FINITE ELEMENT METHOD

5

Table 2. Comparison Test—Analysis for Test Device.

			Tests			Measured	Calculated	
Test #	Flange	Seal	Medium / essure	# of Flange Bolts 009	# of Clamping Ring Bolts 008	Eigenfrequen- cies [Hz]	Eigenfrequen- cies [Hz]	Difference [%]
1	smooth	none	none	12	16	507.02	501.00	-1.20
2					12	504.26	497.30	-1.40
3					8	501.35	493.60	-1.57
4					4	491.73	487.40	-0.89
5					0	480.41	480.40	0.00
6				12	16	506.20	501.00	-1.04
7				6		490.83	481.43	-1.95
8				4		470.43	474.90	0.94
21		graphite profile seal	none	12	16	543.03	536.50	-1.22
22					12	543.76	533.96	-1.84
23					8	544.06	530.57	-2.54
24					4	541.44	528.88	-2.37

BARREL PUMP

Full Finite Element Model

A finite element model of a complete barrel pump was created according to the modeling rules derived from the test device, described above. The pump was selected for this purpose, as most of its components were modeled with finite elements during the design process of this 28 MW high pressure injection pump. A section view of the finite element model is shown in Figure 11. It contains about 107,000 elements with 173,000 nodes. The geometry is meshed with 10-noded tetrahedron elements with quadratic interpolation. Additional elements are beam elements, simulating the bolts of the clamping pieces at the drive-end. Beam elements are applied also at the feet lower surfaces, where the boundary conditions are applied, and are used to stiffen the feet against local deformation at these discrete nodes. Additional elements are linear springs as well, located at positions of unknown stiffness at the following three positions, which are essential for the bearing housing behavior (Figure 11):
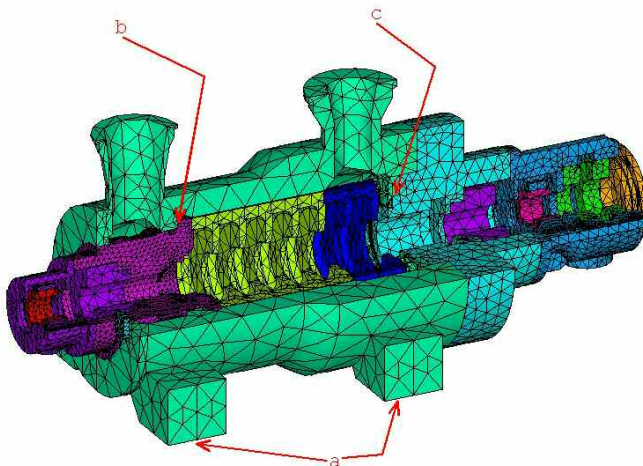

Figure 11. Finite Element Model of Injection Pump.

a. At the feet with different stiffness in the three principal longitudinal directions. These springs simulate the baseplate stiffness. Rotational stiffness is neglected, as it is imposed by a pair of springs at neighbored feet. At each foot the same stiffness values are applied. These values were assumed in a first step and the finite element model of a baseplate obtained them. They have to be adjusted by tests on the real pump.

b. Between suction casing and barrel at the internal shoulder. With this pump design the cartridge is tied against this shoulder by the bolts of the clamping pieces. The contact pressure at this shoulder is increased during operation due to internal pressure. The stiffness values are different in the normal and tangential direction and have to be adjusted by tests on the real pump.

c. Between the last stage casing and the cover. There is a radial loose fit in between these parts, but it is radially guided. Only a normal stiffness is applied, no tangential. This stiffness value has to be adjusted by tests on the real pump.

For the analysis damping is neglected. This means that the finite element program computes only normal eigenvalues. Table 3 shows the results of the analysis up to 600 Hz. Figures 12 to 15 show the bearing housing vibrations in-phase, out-of-phase, vertical, and horizontal. While the first six modes show rigid body motions of the pump, and the following two modes describe cartridge vibration, the modes no. 9 to 12 at about 304 Hz and 376 Hz are the four most interesting eigenvalues. Higher natural frequencies are of interest only for comparison with measured eigenvalues in a later stage.

Table 3. Finite Element Analysis Results of Full Pump.

| Mode #	Freq. [Hz]	Description
1	47.71	Rocking about horizontal y-axis, rigid body motion
2	49.48	Rocking about longitudinal x-axis, rigid body motion
3	78.69	Rocking about vertical z-axis, rigid body motion
4	84.65	Vertical vibration NDE side, stage casings in phase
5	113.69	Vertical vibration DE side, stage casings out of phase
6	145.73	Barrel rocking about longitudinal x-axis, stage casings horizontal vibration
7	158.14	Vertical rocking of cartridge
8	160.12	Horizontal rocking of cartridge
9	304.07	**In phase vertical mode of bearing housings, maximum amplitude at NDE**
10	304.81	**In phase horizontal mode of bearing housings, maximum amplitude at NDE**
11	375.59	**Out of phase vertical mode of bearing housings, maximum amplitude at DE**
12	375.96	**Out of phase horizontal mode of bearing housings, maximum amplitude at DE**
13	415.40	Torsion of inner cartridge, horizontal vibration suction nozzle
14	469.96	Axial vibration of inner cartridge and suction nozzle
15	486.57	Axial vibration of suction nozzle
16	512.76	Horizontal vibration suction nozzle
17	553.42	Horizontal bending barrel, horizontal inner cartridge bending in phase
18	564.21	Vertical bending inner cartridge
19	569.69	Horizontal bending barrel, horizontal inner cartridge bending out of phase
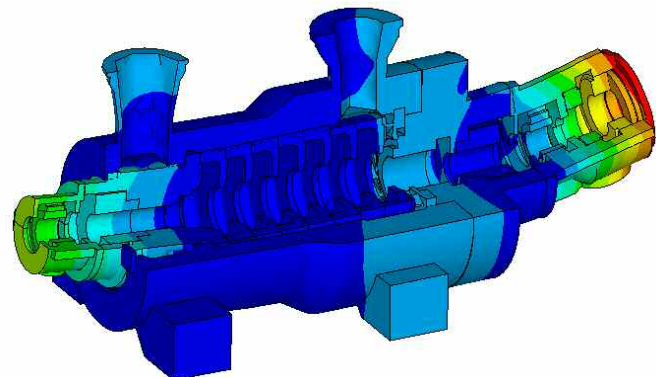
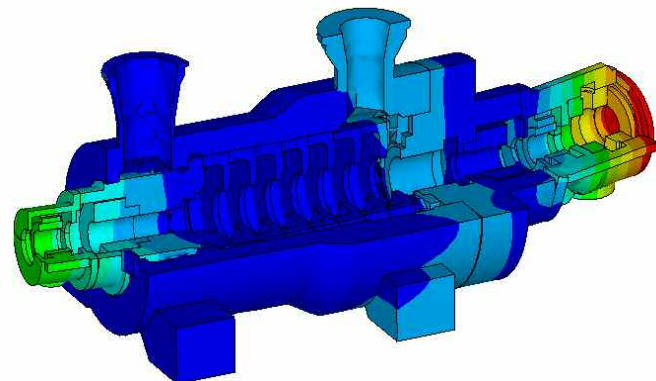*Figure 12. NDE Vertical Mode, Both Ends In-Phase.*

Figure 13. NDE Horizontal Mode, Both Ends In-Phase.

Vertical vibrations of the bearing housing occur as well at lower frequencies (mode 4 and 5), but these frequencies seem to depend a lot on the stiffness of the springs, simulating the baseplate. So, in a next step different boundary conditions were applied at the feet to look at the influence of these stiffness values:
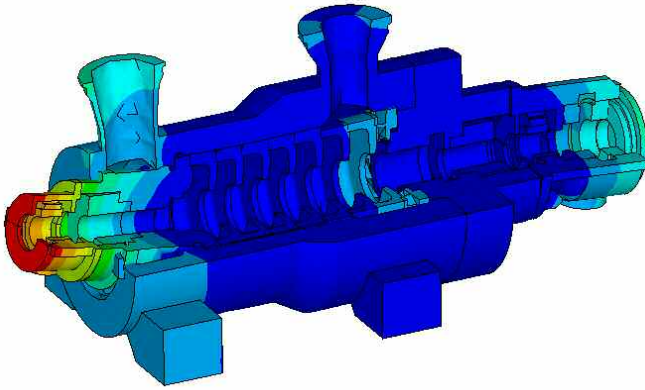
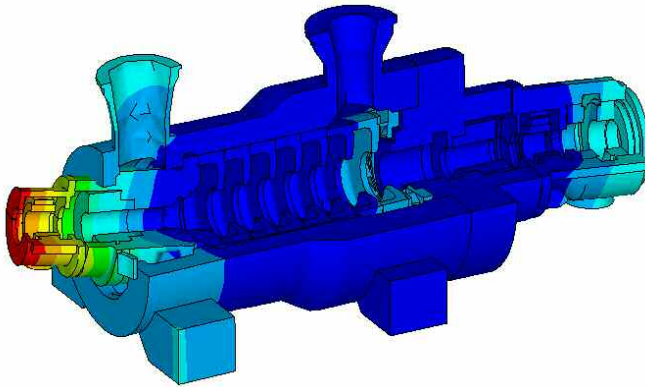*Figure 14. DE Vertical Mode, Both Ends Out-of-Phase.*

Figure 15. DE Horizontal Mode, Both Ends Out-of-Phase.

• No boundary conditions are applied at the feet at all, the so-called free-free condition

• The above-mentioned springs are applied simulating the baseplate.

• An about 100 times higher spring stiffness is applied at the feet.

• The feet are constrained in all three directions of space at their feet.

The influence of these boundary conditions on the drive-end and nondrive-end natural frequencies is shown in Figure 16. The results of the model on springs simulating the baseplate are selected as the reference. The free-free model results in a little bit lower frequency, but still acceptable. The difference is 2.5 percent in maximum. The differences between the very stiff baseplate springs and the constrained boundary conditions are negligible, the natural frequencies calculated are up to 25 percent higher for the vertical modes. For the horizontal modes the increase is only about 3.5 percent. This means that the feet and barrel stiffness in between is not negligible for the determination of the eigenvalues. Additionally the natural frequencies of the following models are included in this diagram:

• Drive-end bearing housing alone. This model contains the suction housing and the clamping plates with their bolts as well. It is constrained at the shoulder of the suction housing plus at the contact areas of the clamping plates at the barrel.

• Nondrive-end bearing housing alone. It is constrained at the contact areas of the bolts toward the cover.

• Nondrive-end bearing housing plus the cover. It is constrained at the contact area of the cover toward the barrel.

The single models result in higher frequencies as the reference. This is due to the constraints of these models. The difference is up to 20 percent. Therefore the single models alone are incomplete to determine the natural frequencies analytically. The NDE model
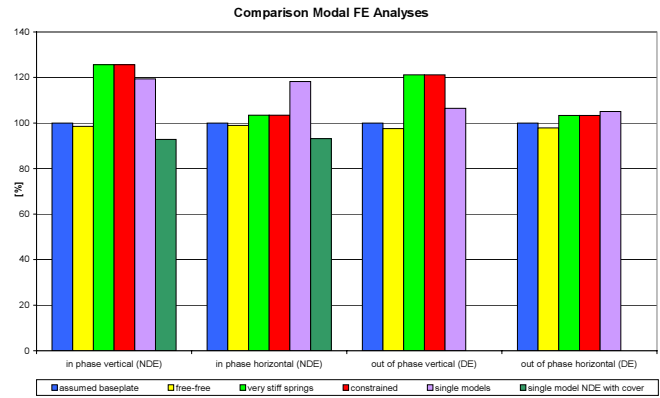

Figure 16. Bearing Housing Natural Frequencies Depending on Baseplate Stiffness (A).

with the cover shows up to 8 percent lower natural frequencies, although it is constrained at the cover flange. Thus the cartridge must have an additional supporting influence. Whether this kind of model could be used to determine the NDE natural frequencies depends on the pedestal stiffness.

Figure 17 shows how selected modes depend on the pedestal stiffness. Selected are the modes #4, 5, 9, 10, 11, 12, 15, and 16 from Table 3. The first two show a vertical bearing housing vibration as well, but together with a motion of the whole barrel. The last two modes are suction nozzle modes, whose mode shape could be easily identified by experimental modal analysis. With increasing spring stiffness at the feet, up to fully constrained, all the natural frequencies of these modes increase, with the exception of the highest suction nozzle mode. The main increase for all modes is between the assumed baseplate stiffness and very stiff springs. The pure bearing housing modes are not that sensitive to baseplate stiffness. The modes where the whole pump is involved are very sensitive on this parameter.
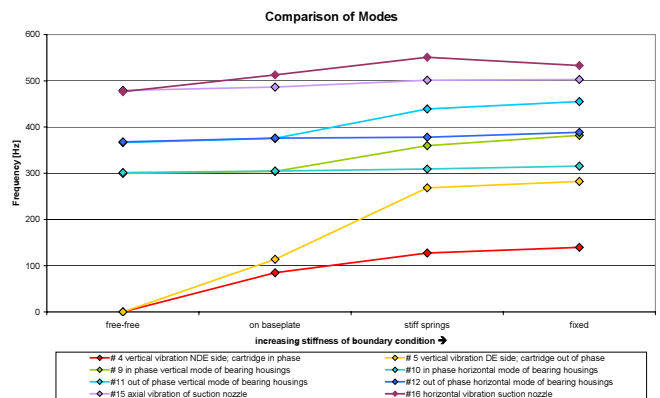

Figure 17. Bearing Housing Natural Frequencies Depending on Baseplate Stiffness (B).

Modal Tests

The modal tests were performed at the pump on its baseplate similar to the tests at the test device. A number of 15, biaxial accelerometers were placed on the outer surface of the pump; accelerometers could not be placed at the cartridge, as it was not accessible. The accelerometers were used to make measurements in two orthogonal directions at each location, as listed in Table 4.

The numbers correspond to a simplified mesh of the pump hull (Figure 18) created to identify the measurement points and to have correct distances for interpolating the motions in the measurement system. To create this mesh, which replaces the two simple beams of the test device model, an initial graphics exchange specification

IDENTIFICATION OF BEARING HOUSING VIBRATIONS OF A LARGE BARREL TYPE
INJECTION PUMP AND THEIR ANALYSIS BY MEANS OF THE FINITE ELEMENT METHOD

7

Table 4. Accelerometer Positions and Directions.

No.	Location	1st Direction	2nd Direction
62	NDE bearing housing outboard top	Horizontal lateral Y	Vertical X
282	NDE bearing housing outboard side	Horizontal lateral Y	Vertical X
221	NDE bearing housing inboard side	Horizontal lateral Y	Vertical X
218	NDE bearing housing inboard top	Horizontal lateral Y	Vertical X
475	DE bearing housing outboard top	Horizontal lateral Y	Vertical X
30	DE bearing housing inboard side	Horizontal lateral Y	Vertical X
368	DE bearing housing inboard top	Horizontal lateral Y	Vertical X
113	DE bearing housing outboard side	Horizontal lateral Y	Vertical X
181	Suction nozzle side	Horizontal lateral Y	Horizontal axial Z
28	Discharge nozzle side	Horizontal lateral Y	Horizontal axial Z
231	Pump foot drive end left	Horizontal lateral Y	Vertical X
96	Pump foot drive end right	Horizontal lateral Y	Vertical X
242	Pump foot non drive end right	Horizontal lateral Y	Vertical X
435	Pump foot non drive end left	Horizontal lateral Y	Vertical X
417	Hammer position middle of barrel 45°	Horizontal lateral Y	Vertical X

(IGES) file was written out of the finite element preprocessor and read in the data acquisition system. This datum acquisition system consists of a 17-channel signal conditioning unit and a notebook personal computer (PC) with the appropriate software. The accelerometers and the instrumented hammer were connected to this measurement system. An impact point at the middle of the pump case, and at an angle of 45 degrees to the horizontal, was selected in order to excite all parts of the structure in both vertical and horizontal planes. Some initial tests indicated that it was difficult to get enough vibration energy into the heavy pump from a single impact, although the heaviest available hammer (1.4 kg) was selected. However, the signal analysis software was designed also for other methods of excitation, and, by using the hammer to simulate a shaker with random input, it was possible to produce an adequate vibration response from the structure (Figure 19). The levels of excitation and vibration were monitored during the tests and the software was set up to reject bad data automatically.
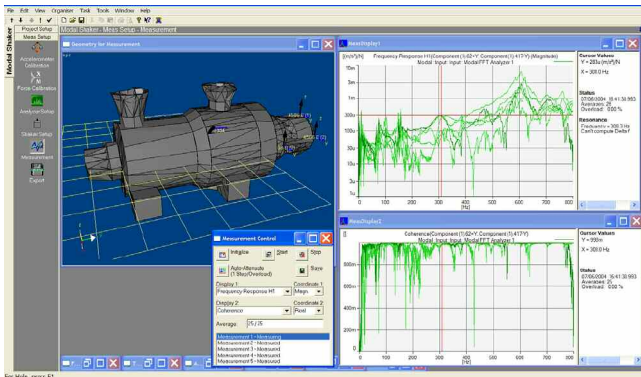

Figure 18. Data Acquisition System with Figure of Measurement Mesh of Pump.

A contour map (Figure 20) shows the mobility of the pump structure. This is a plot of the average frequency response H1 (acceleration/force) at each measurement position, and it shows more activity at the higher frequencies because it is based on acceleration measurements. Contrary to the numerical solution, where there were sharp discrete eigenvectors with their natural frequencies, there is now response at all frequencies and the eigenvectors merge into each other, an outcome of the damping in the structure. Where several of the measurement locations indicate high amplitudes, a natural frequency of those parts of the structure is likely. Additional specialized software allowed the responses at discrete, selected frequencies to be analyzed and indicate the motion of the structure, by interpolating from the measured vibration to other points of the mesh (Figure 21). Table 5 shows extracted frequencies, so called "operational deflection shapes" (ODS). They show how the structure deforms at certain frequencies. If the eigenvectors do not influence each other too much, they are nearly identical with the natural frequencies.
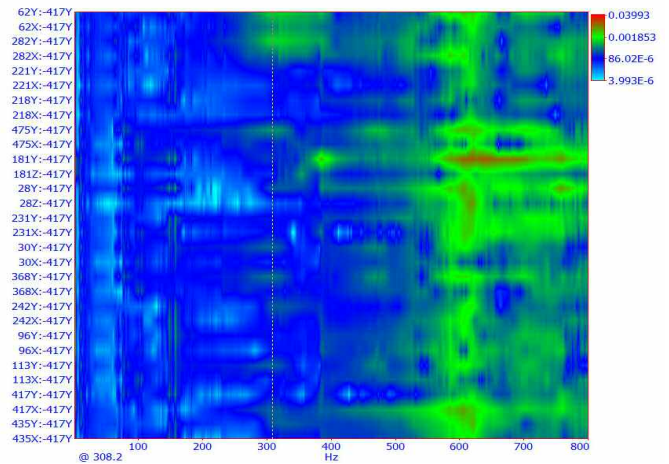

Figure 19. Performing the Hammer Tests.

Figure 20. Average Frequency Response H1 at Each Measurement Position.
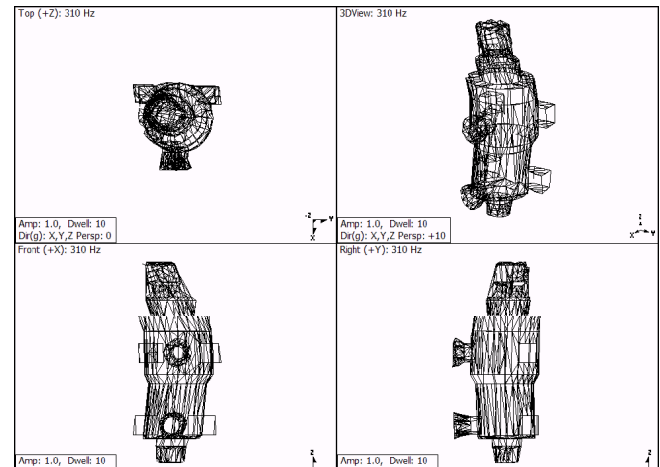
Figure 21. Interpolated Mode Shape.

Table 5. Extracted Eigenvectors.

Mode #	Frequency [Hz]	Description
1	8.25	Axial rigid body motion of pump
2	9.50	Lateral rigid body motion of pump
3	76.75	Lateral rocking of pump
4	95.00	Axial rocking of pump
5	98.75	Axial rocking of pump
6	104.00	Axial rocking of pump
7	148.00	Torsional rocking of pump
8	157.00	Torsional rocking of pump
9	285.00	Diagonal 1st bending of pump, bearing housings in phase
10	310.00	Diagonal 1st bending of pump, bearing housings in phase
11	318.50	Diagonal 1st bending of pump, bearing housings in phase
12	355.00	Horizontal NDE bearing housing vibration, axial suction nozzle
13	385.00	Horizontal vibration suction nozzle
14	470.00	Diagonal 2nd bending of pump, bearing housings out of phase
15	527.00	Diagonal 2nd bending of pump, bearing housings out of phase
16	585.50	Torsion of barrel

It has to be mentioned that also on those eigenvectors described as rigid body motion, there is always some relative motion in the pump model due to measurement noise. The number of measurement points is not sufficient to describe the eigenvectors and, due to this, the interpolation gives unlikely results. This can be seen at mode #12 (355 Hz). There are only two axial measurements: at the suction nozzle and the discharge nozzle. While an axial vibration at the suction nozzle is measured, the discharge nozzle remains quiet. The interpolation leads to an axial stretching of the whole barrel and not alone to an axial bending of the suction nozzle, which is the much more likely behavior. Additional tests with many more measurement points, also at the cartridge, have to be carried out to obtain a more realistic behavior. These measurements are on their way. Furthermore a curve fitting software would be good to determine the natural frequencies. Although the existing software gives additional guidance to the contour plots, i.e., the response functions at a certain point and direction with the possibility to look for peak values in these curves, the curve fitting software would result in the clear damped natural frequencies.

On the other hand some clear coincidences with the finite element analysis have been found. At lower frequencies we observe the rigid body motions of the pump on its pedestal. Between 300 Hz and 400 Hz we observe the bearing housing vibrations, as calculated. And at higher frequencies, the nozzles start to vibrate. By a correlation the parameters of the finite element model should be updated to meet the measurement results.

Correlation Analysis

The correlation analysis is performed in a software tool, which can read in finite element models as well as the measured results. It is important to have the same coordinate system and origin. This was guaranteed by the export of the finite element geometry to the data acquisition system. The measurement mesh and the eigenvectors and—frequencies were exported by universal files and read into the correlation software. Some difficulties occurred within the use of this software. The result files produced by the finite element code were too large to be read in directly. Only the model itself could be read in and the solver within the correlation software could be used to obtain the eigenvalues. But this solver cannot handle 10-noded tetrahedron elements, so the whole model was converted to four-noded tetrahedrons with a linear interpolation, which have the great disadvantage of being much too stiff in their bending behavior. The stiffness increase due to the different element formulation is up to 30 percent. This led to an increase of natural frequencies, especially of the bearing housing modes, where bending plays an important role. The rigid body modes were not affected that much. This was a large disadvantage of the applied software tool and this fault should be corrected in the next releases of this software.

Within this software test and analysis are compared by the so-called "modal assurance criterion" (MAC) according to Blakely and Rose (1993), which is defined by the eigenvectors of test and analysis for each pair of analytical and test mode shape:

$$MAC_{ij} = \frac{\left(\left(\phi_t^T \right)_i \cdot \left(\phi_a^T \right)_j \right)^2}{\left(\phi_t^T \cdot \phi_t \right)_i \cdot \left(\phi_a^T \cdot \phi_a \right)_j} \tag{1}$$

where:

ϕ_a = Analytical mode shape vector reduced to the test degree of freedoms

ϕ_t = Test mode shape vector

Its value ranges from zero (no correlation between shapes) to one (full correlation) or 100 percent. The MAC compares pair with the mode shapes independent of frequency. The MAC-matrix of the first 16 eigenvalues experimentally (EMA) and computational (FEA) is shown in Figure 22. It shows that the highest conformance is along the diagonal. Ideal would be a matrix where only the diagonal elements show very high conformance values of 100 percent; out-of-diagonal elements are negligible. Table 6 shows the best correlations found. This table shows a coincidence in mode shapes, but not in frequencies. The best coincidence is found for the torsional rocking of the pump at 157 Hz. Very good coincidence was found also for the horizontal vibration of the suction nozzle (385 Hz), the in-phase bearing housing vibration (310 Hz), and the axial rocking of the pump (98.75 Hz).
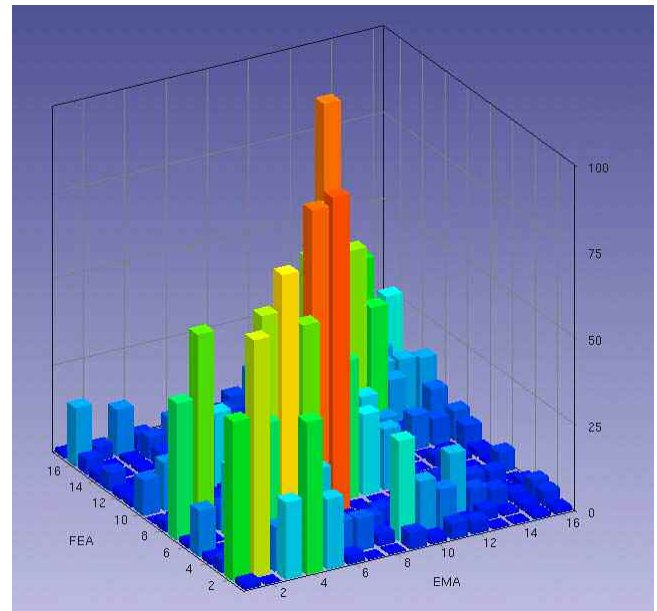

Figure 22. MAC Before Optimization.

Table 6. MAC of Selected Pairs.

Pair #	FEA		EMA		Frequency Diff. [%]	MAC [%]
	Mode #	Freq. [Hz]	Mode #	Freq [Hz]		
1	1	48.70	4	95.00	-48.73	44.1
2	2	50.29	2	9.50	429.39	68.3
3	3	81.34	3	76.75	5.98	40.3
4	5	117.38	5	98.75	18.87	75.7
5	6	150.24	8	157.00	-4.31	91.3
6	7	193.43	9	285.00	-32.13	40.2
7	8	195.35	6	104.00	87.84	38.5
8	10	344.87	10	310.00	11.25	75.8
9	16	587.99	13	385.00	52.73	87.5

Table 6 shows a coincidence in mode shapes, but not in frequencies. For example there is a high correlation at pair #2, the lateral rigid body rocking of the pump. At the finite element analysis the frequency is determined by the springs at the feet modeling the baseplate. It is assumed that this baseplate is fixed at its base location. In reality this baseplate was not fixed to the base

IDENTIFICATION OF BEARING HOUSING VIBRATIONS OF A LARGE BARREL TYPE
INJECTION PUMP AND THEIR ANALYSIS BY MEANS OF THE FINITE ELEMENT METHOD

9

of the shop floor, where the tests were performed. Another good correlation is at pair #8. The difference in frequency can be explained by the usage of the four-noded tetrahedrons, resulting in 345 Hz, rather than the 10-noded elements, where this mode shape was at 304 Hz. The latter fits much better to the measured 310 Hz.

So in a next step finite element model parameters were changed to obtain a better coincidence. These parameters are the selected stiffness values for the applied spring elements as well as the Young's modulus of the solid elements, one Young's modulus per part. Ratings of confidence are given for these parameters, in general for the Young's modulus a range of ±20 percent was set for the cast parts and ±10 percent for the forged parts. By a sensitivity analysis those parameters with the highest impact were selected for the optimization to reduce the number of parameters.

The MAC-matrix with this optimized finite element model is shown in Figure 23 and in Table 7. It shows nearly the same coincidence as the previous matrix with nonoptimized parameters for all pairs; only the in-phase bearing housing vibration is nearly identical now. The highest changes in values were made at the stiffness values of the pedestal springs. In the vertical direction it was decreased by 19 percent, in the lateral direction it was increased by 44 percent, and in the axial direction it was decreased by 63 percent. As too stiff four-noded tetrahedrons were used in the analysis, the Young's modulus of the barrel and NDE bearing housing had to be adjusted by −21 percent and −31 percent, respectively, to correct this effect.
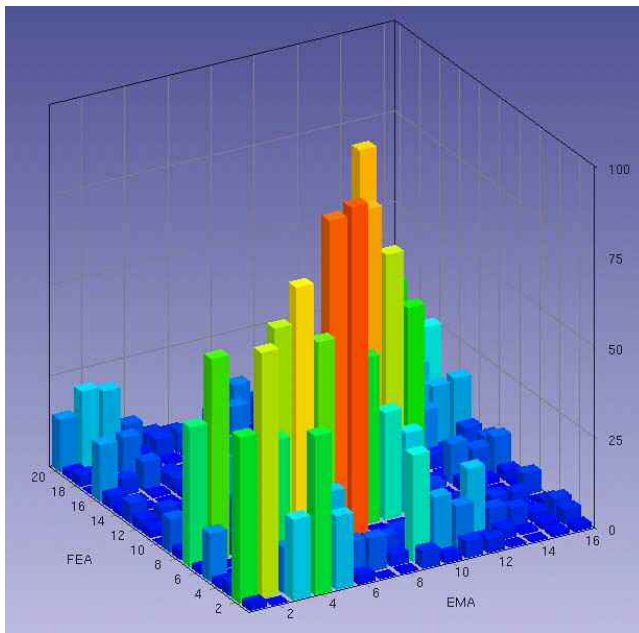

Figure 23. MAC After Optimization.

Table 7. MAC of Selected Pairs After Optimization.

Pair #	FEA		EMA		Frequency Diff. [%]	MAC [%]
	Mode #	Freq. [Hz]	Mode #	Freq [Hz]		
1	1	48.76	4	95.00	-48.68	44.0
2	2	50.63	2	9.50	429.97	68.0
3	3	81.88	3	76.75	6.68	40.3
4	5	117.51	5	98.75	18.99	75.5
5	6	151.54	8	157.00	-3.48	91.1
6	7	194.47	9	285.00	-31.76	44.5
7	8	196.32	6	104.00	88.77	36.0
8	9	309.54	10	310.00	-0.15	81.6
9	16	587.99	13	385.00	52.73	83.2

The optimization study is not complete yet. More parameters must be adapted. However, it can be emphasized that the correlation already obtained between a few EMA-FEA mode shapes can be regarded as quite satisfactory.

CONCLUSIONS

By means of the test device modeling criteria for the assembly of pumps were defined to obtain realistic results of modal analyses. A three-dimensional finite element model of an injection barrel pump was created and the natural frequencies with their mode shapes determined. This produced several results. First the bearing housing vibration is not a vibration of the bearing housing. Depending on the frequency of interest, more or less of the pump is affected in this vibration. For lower modes, the pedestal stiffness is important for the vibration. Higher modes, where the bearing housings are vibrating, depend less on this stiffness.

The experimental modal analysis of the pump produced similar results. There are some modes at lower frequency. The in-phase vibration of the bearing housings alone was measured at a similar frequency (310 Hz) as calculated (304 Hz). The out-of-phase vibration could not be detected and with higher frequencies a coincidence between test and calculation could not be seen at first glance. The tests had two deficits. First the number of measurement points was too low to allow a proper interpolation of the measured points onto the whole pump. Second the software was not able to allow curve fitting for an extraction of the eigenvalues; only the operational deflection modes at certain frequencies could be measured.

To close the gap between the test and calculation a correlation analysis was performed. The correlation of the mode shapes, shown in a modal assurance criterion matrix, was fairly good. But with more measurement points it could be improved, as the interpolation from the measurement points to the entire surface of the pump would be improved. In a second step assumed properties of the finite element model were optimized to obtain a better modal assurance criterion matrix. The main deficit in the correlation analysis was the fact that a transfer of the results from the finite element system to the correlation analysis was not possible, because the model was too large. Elements with a too stiff formulation had to be used instead of the original elements, resulting in wrong frequencies. So the frequency coincidence was not as good as the mode shape coincidence.

Additional work has to be done. More measurement points have to be taken into account at the tests, and it would be good to have the curve fitting software module to obtain the mode shapes and their frequencies out of the experimental modal analysis. For the correlation a way must be found to consider large finite element models with free tetrahedron meshes. But nevertheless this examination has increased the knowledge of bearing housing vibrations and the results are quite encouraging. Especially the small difference between the measured and the calculated first pure in-phase bearing housing vibration is a great success, and the numerical prediction of these vibrations due to vane passing frequency is in reach.

For the actual pump the results obtained are positive. As this pump has seven vane impellers and it will operate between 4200 and 4800 rpm, natural frequencies of the bearing houses should be avoided between 392 Hz and 672 Hz, including a separation margin of 20 percent. As the measured and tested natural frequencies are below this range, a resonance situation should not occur.

REFERENCES

API Standard 610, 2003, "Centrifugal Pumps for Petroleum, Petrochemical and Natural Gas Industry," Ninth Edition, American Petroleum Institute, Washington, D.C.

Blakely, K. and Rose, T., 1993, "Cross-Orthogonality Calculations for Pre-Test Planning and Model Verification," MSC World User's Conference, MacNeal Schwendler Corporation, Los Angeles, California.

Dascotte, E., 2004, "Linking FEA with Test, Sound and Vibration," Bay Village, Ohio.

VDI 2230, 2003, "Systematic Calculation of High Duty Bolted Joints—Joints with One Cylindrical Bolt," Verein Deutscher Ingenieure e.V., Düsseldorf, Germany.